nature physics

Article

https://doi.org/10.1038/s41567-023-01979-8

Intrinsic spin Hall torque in a moiré Chern magnet

In the format provided by the authors and unedited

SUPPLEMENTARY MATERIALS

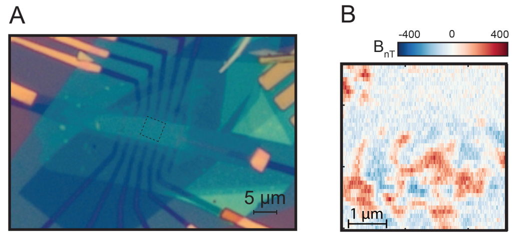

Fig. S1. **NanoSQUID imaging at $\nu = -1$ on monolayer $MoTe_2$/monolayer WSe_2 device.** (**A**) Optical image of a monolayer $MoTe_2$/monolayer WSe_2 device. (**B**) NanoSQUID imaging revealed qualitatively similar magnetism and anomalous Hall resistances in this device. This device was rather disordered and did not show quantization of anomalous Hall resistance.

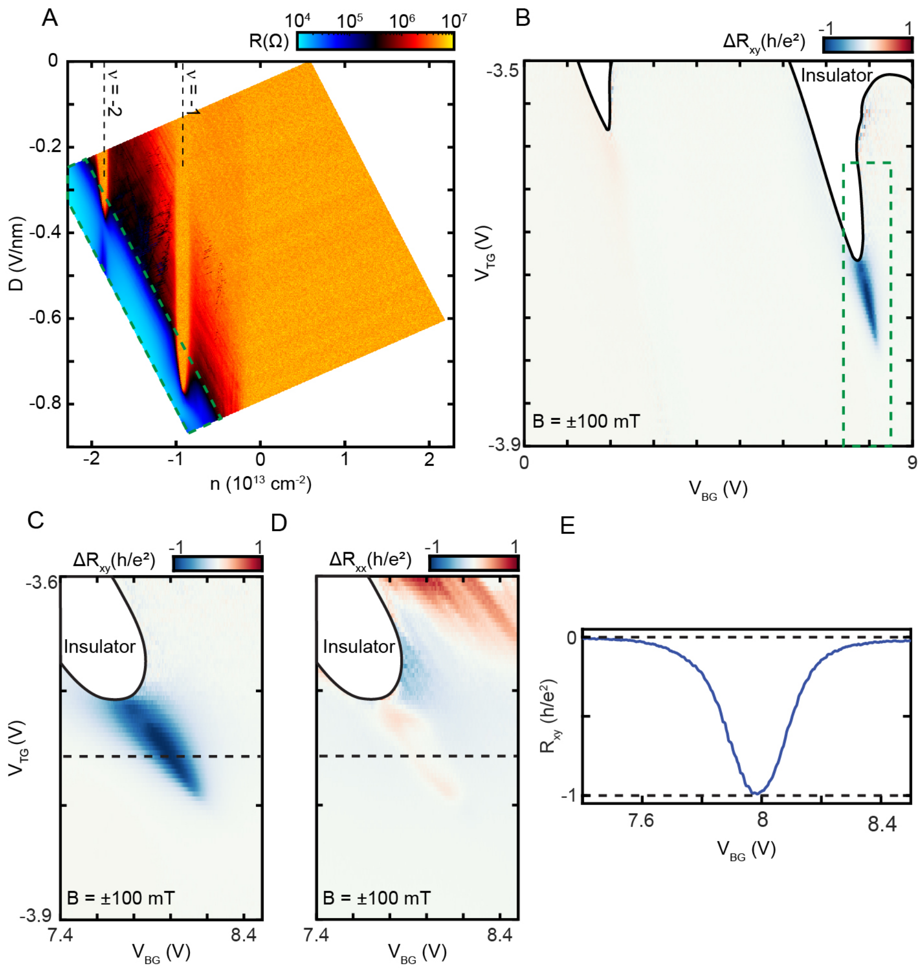

Fig. S2. **Phase diagram from transport data** (**a**) Two terminal resistance of device (measured between contacts *abcd* and j) plotted as a function of electron density n and displacement field D, where $D = \frac{V_{TG}-V_{BG}}{d_t+d_b}$, $n = \epsilon\epsilon_0(V_{TG}/d_t + V_{BG}/d_b) + n_0$. Here $d_t = 2.7$ nm is the thickness of the top hBN layer, $d_b = 12.1$ nm is the thickness of the bottom hBN layer, $\epsilon \approx 3$ is the relative dielectric constant of hBN, and n_0 is the offset charge carrier density, 5.9×10^{12} cm^{-2}. At low displacement fields $\nu = -1$ and $\nu = -2$ both host topologically trivial insulating states, with the $\nu = -1$ insulator presumably interaction-driven. In the electron-doping regime large contact resistances hamper transport measurements. (**b**) ΔR_{xy} measurement in the region inside the green dotted line in **a**. A finite ΔR_{xy} appears near $\nu = -1$ in a narrow range of D. (**c**) ΔR_{xy} measurement in the region inside the green dotted line in **b**. Precise quantization of ΔR_{xy} obtains over a range of displacement fields at $\nu = -1$. (**d**) Symmetrized R_{xx} measurement in the region inside the dotted line in **b**. (**d**) Linecut of ΔR_{xy} along the dotted line in **c** illustrating the appearance of a QAH effect.

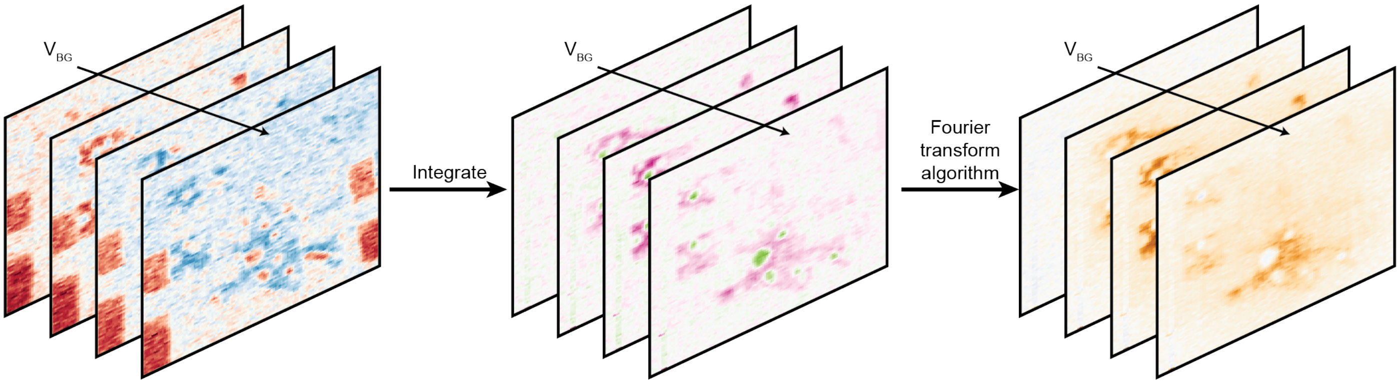

Fig. S3. **AC bottom gate conversion to magnetization.** (**a**) AC bottom gate magnetometry produces $\delta B_z/\delta V_{BG}(x, y, V_{BG})$. (**b**) We integrate $\delta B_z/\delta V_{BG}(x, y, V_{BG})$ with respect to V_{BG} to obtain $B_z(x, y, V_{BG})$ (**c**) For each value of V_{BG} we invert $B(x, y)$ to produce $m_z(x, y, V_{BG})$, which is presented as a video of the out-of-plane magnetization as V_{BG} enters and then leaves the QAH regime in the supplementary data.

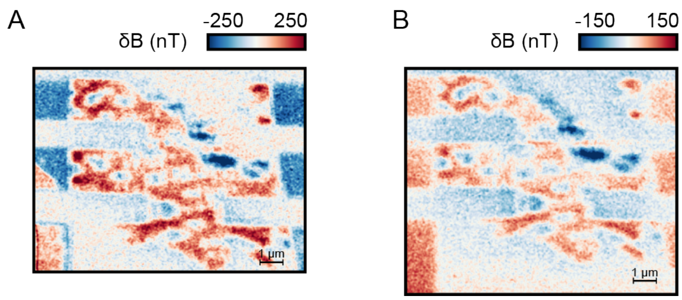

Fig. S4. **Repeated cooldowns** (**a**) Magnetic structure measured at 28 mT, $V_{TG} = -3.734$ V, $V_{BG} = 7.818$ V at a height of 125 nm with nanoSQUID diameter $\phi = 159$ nm. (**b**) Magnetic structure measured at 36 mT, $V_{TG} = -3.756$ V, $V_{BG} = 7.943$ V during a subsequent cooldown at a height of 175 nm with nanoSQUID diameter $\phi = 113$ nm.

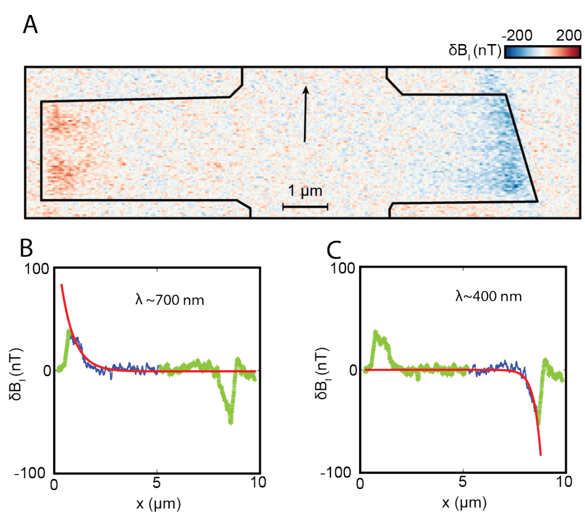

Fig. S5. **Spin diffusion length** (**a**) Spin Hall effect near $\nu = -1$ (**b**) Fit of the left edge. Green regions are masked from the fit, blue is fit to an exponential decay function, $B(x) = A \cdot e^{-\frac{x}{\lambda}} - c$. Approximate spin diffusion length λ is 700 nm. (**c**) Fit of the right edge, approximate spin diffusion length λ is 400 nm.

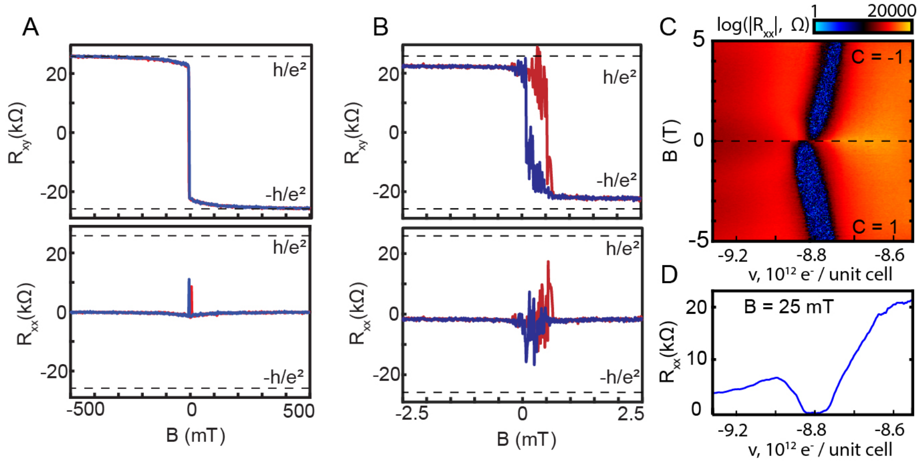

Fig. S6. **Additional transport properties of the magnetic Chern insulator** (**a**) Magnetic hysteresis loop in QAH regime. At ±500 mT quantization reaches $1.000 \pm 0.006\ h/e^2$ and $-0.996 \pm 0.005\ h/e^2$. (**b**) Close to $B = 0$ $R_{xy} \approx 0.9\ h/e^2$. Coercive fields are less than 1 mT at the measurement temperature of 1.6K. (**c**) Dependence of the degeneracy of the Chern band on B reveals the Chern number of the ground state at finite field, which is -1 in this system. (**d**) Linecut shows R_{xx} reaches $-93\ \Omega$ ± 115 Ω.

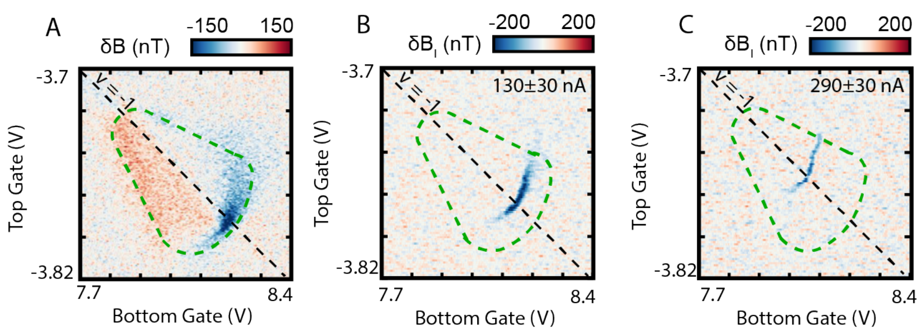

Fig. S7. **Current-switching phase diagram** (**a**) Bottom gate modulation magnetometry phase diagram taken at the point at which measurements for Fig. 4g were performed. The green dotted outline appears in that figure. $\delta V_{BG} = 35$ mV was used. (**b**) Current-induced magnetic domain switching signal δB_I as a function of top and bottom gate voltages with $I_{SD} = 130$ nA, $\delta I_{SD} = 30$ nA. (**c**) The same measurement with $I_{SD} = 290$ nA, $\delta I_{SD} = 30$ nA. Magnetic switching appears over broad regions of the magnetic phase diagram, although currents required to effect domain switching vary with gate voltages.